http://dx.doi.org/10.5012/bkcs.2013.34.2.415

Chemical Substitution Effect on Energetic and Structural Differences between Ground and First Electronically Excited States of Thiophenoxyl Radicals

Jun-Ho Yoon, Jeong Sik Lim,[a] Kyung Chul Woo, Myung Soo Kim,[†] and Sang Kyu Kim[*]

Department of Chemistry, KAIST, Daejeon 305-701, Korea. [*]E-mail: sangkyukim@kaist.ac.kr
[†]School of Chemistry, Seoul National University, Seoul 151-742, Korea
Received October 28, 2012, Accepted November 12, 2012

Effect of chemical substitution at the *para*-position of the thiophenoxyl radical has been theoretically investigated in terms of energetics, structures, charge densities and orbital shapes for the ground and first electronically excited states. It is found that the adiabatic energy gap increases when CH_3 or F is substituted at the *para*-position. This change is attributed to the stabilization of the ground state of thiophenoxyl radical through the electron-donating effect of F or CH_3 group as the charge or spin of the singly-occupied molecular orbital is delocalized over the entire molecule especially in the ground state whereas in the excited state it is rather localized on sulfur and little affected by chemical substitutions. Quantitative comparison of predictions based on four different quantum-mechanical calculation methods is presented.

Key Words : Substitution effect, Thiophenoxyl, Spin distribution, Chemical energetics

Introduction

Recent studies on the πσ* mediated photodissociation dynamics have revealed many interesting facets of multi-dimensional conical intersection seam through which non-adiabatic transitions become facilitated effectively. The first electronically excited state corresponding to the ππ* transition is bound in nature whereas an upper-lying πσ* state is repulsive along a specific chemical bond. In this way, potential energy surfaces of the excited states are forced to be crossed at particular nuclear configurations, generating a multi-dimensional conical intersection seam along the photodissociation reaction pathway. This type of excited state dynamics is frequently met in a number of photochemical pathways as π conjugated systems coupled with a heteroatom such as oxygen, nitrogen, or sulfur are quite ubiquitous in many fields of chemistry and biology. These include phenol,[1-3] anisole,[4,5] aniline,[6,7] pyrrole,[8-10] thiophenol,[2,11-13] and thioanisole,[14] giving rise to H or CH_3 fragment upon UV excitation as the X-H(CH_3) bond dissociation takes place (X = O, N, or S) along the repulsive πσ* state. Bond dissociation dynamics is very sensitive to the electronic/nuclear coupling mechanism at nuclear configurations constructing the reaction coordinate, and thus chemical substitutions on the aromatic ring moiety could induce significant effects on the whole chemical reaction dynamics as the π conjugation of the aromatic ring moiety which may be sensitive to the chemical substitution should modify potential energy surfaces in terms of energetics and morphology.

In this respect, we studied here chemical substitution effect on the thiophenoxyl radical in the ground and first electronically excited states. From the recent photodissociation dynamics studies on thiophenols[2,11-13] and thioanisoles,[14] it has been found that the thiophenoxyl radical is produced either in the ground state, $C_6H_5S\cdot$ ($\tilde{X}$), or in the first electronically excited state, $C_6H_5S\cdot$ ($\tilde{A}$). Relative yields of two competing reaction channels are governed by the nonadiabatic transition probability of the reactive flux at the conical intersection seam. Experimentally, using velocity-map ion imaging or Rydberg-tag technique, one could precisely estimate the branching ratio between these two channels as the small but distinct energy gap between $C_6H_5S\cdot$ ($\tilde{X}$) and $C_6H_5S\cdot$ ($\tilde{A}$) allows separation of two adiabatic channels in the total translational distribution of products. The adiabatic energy gap between $C_6H_5S\cdot$ ($\tilde{X}$) and $C_6H_5S\cdot$ ($\tilde{A}$) was precisely measured to be 0.3719 eV by the Neumark group,[15] and this is quite consistent with theoretical predictions calculated by Lee *et al*. some time ago.[16] The $\tilde{A}$-$\tilde{X}$ energy gap of the thiophenoxyl radical is very small for the energy difference between two electronic states, which could be attributed to the poor conjugation of nonbonding orbital of sulfur (3*p*) with the π orbital (2*p*) of the benzene moiety.[17] Therefore, it is a natural question how the energy gap between *p*-Y-$C_6H_4S\cdot$ ($\tilde{X}$) and *p*-Y-$C_6H_4S\cdot$ ($\tilde{A}$) will be changed as the electron donating or withdrawing Y group is substituted instead of H. Though the substitution effect on the S-H bond dissociation energy of thiophenols had been previously studied,[18-23] those studies were naturally focused only on the ground state of the thiophenoxyl radical.

Computational Detail

State-averaged complete active space self-consistent field (SA-CASSCF) and density functional theory (DFT) methods were employed for the calculation of the electronically excited states of thiophenoxyl radicals. In the SA-CASSCF, active space of 9 electrons distributed over 8 molecular

[a]Current address: Center for Gas Analysis, Korea Research Institute of Standards and Science (KRISS), Daejeon 305-340, Korea

orbitals was considered whereas aug-cc-pVTZ[24,25] basis set was used in order to depict partial Rydberg character of the excited state. Complete active space second-order perturbation (CASPT2) and cluster-corrected (Davidson correction) multireference configuration interaction (MRCI+Q) are also employed for further consideration of dynamic electron correlation. Geometries of the ground and first excited states were fully optimized by CASPT2 or DFT for the calculations of vertical and adiabatic energy gap between two states and harmonic vibrational frequencies. SA-CASSCF, CASPT2, and MRCI+Q calculations were carried out using MOLPRO[26] whereas Gaussian 09 program[27] was used for DFT calculations and natural bonding orbital (NBO) analyses.[28]

Results and Discussion

Optimized geometry parameters of thiophenoxyl radicals in the ground and excited states, calculated by CASPT2 and DFT, are given in Table 1 for $C_6H_5S\cdot$, *p*-F-$C_6H_4S\cdot$, and *p*-CH_3-$C_6H_4S\cdot$ with corresponding atomic labels depicted in Figure 1. One of notable geometrical differences between ground and excited states of thiophenoxyl radicals is the C-S bond length change. For instance, the C-S bond length of $C_6H_5S\cdot$ is lengthened by 0.041 (0.040) Å in the excited state compared to that in the ground state according to CASPT2 (DFT). Lengthening of C-S bond upon (symmetry-forbidden) electronic excitation also applies to the case of *p*-F-$C_6H_4S\cdot$ and *p*-CH_3-$C_6H_4S\cdot$. Interestingly, the C-S bond length remains more or less same as F and CH_3 groups are *para*-substituted in the excited state whereas it is slightly shortened in the ground state, Table 1. This already suggests that π-conjugation of thiophenoxyl radicals in the excited state is somewhat different from that in the ground state. Other geometrical parameters are little sensitive to the *para*-substitution of F or CH_3, indicating that electron donating effect of F or CH_3 group is not significant enough for inducing structural changes in both excited and ground states of thiophenoxyl radicals.

The most accurate value for the adiabatic $\tilde{A}$-$\tilde{X}$ energy gap of $C_6H_5S\cdot$ is calculated to be 0.367 eV by CASPT2/aug-cc-pVTZ, which is in good agreement with the most recent experimental value of 0.3719 eV.[15] It should be noted that our theoretical result is slightly different from a previously reported value of 0.376 eV by Cheng *et al*.,[16] and this seems to result from the use of two-state averaged reference function for the consideration of electron correlation in this work whereas the single state wave function was used in Ref. 16.

Table 1. Calculated geometry parameters of $\tilde{X}$ and $\tilde{A}$ state of substituted thiophenoxyl radicals obtained at the level of CASPT2 and DFT. Units are angstroms for the bond length and degrees for the angle. See Figure 1 for the representative atom labels

	$C_6H_5S\cdot$		*p*-F-$C_6H_4S\cdot$		*p*-CH_3-$C_6H_4S\cdot$[a]	
	CASPT2	DFT[b]	CASPT2	DFT	CASPT2	DFT
			$\tilde{X}\ ^2B_1/A''$			
r_{1C7S}	1.711	1.723	1.709	1.721	1.708	1.720
r_{1C2C}	1.418	1.414	1.419	1.415	1.419(1.418)	1.415(1.413)
r_{2C3C}	1.388	1.382	1.387	1.381	1.385(1.388)	1.379(1.382)
r_{3C4C}	1.400	1.395	1.393	1.389	1.406(1.403)	1.403(1.400)
r_{2C8H}	1.081	1.080	1.081	1.080	1.081	1.080
r_{3C9H}	1.081	1.081	1.080	1.080	1.083	1.083(1.082)
$r_{4C12(H/F/C)}$	1.081	1.081	1.342	1.343	1.500	1.502
α_{6C1C2C}	118.7	118.4	118.5	118.2	118.1	117.8
α_{1C2C3C}	120.4	120.6	120.9	121.1	120.6	120.8
α_{2C3C4C}	120.1	120.1	118.4	118.5	121.1	121.2
α_{1C2C8H}	118.4	118.6	118.5	118.6	118.4	118.5(118.6)
α_{4C3C9H}	119.9	120.0	119.6	119.7	119.2	119.3
			$\tilde{A}\ ^2B_2/A'$			
r_{1C7S}	1.752	1.763	1.753	1.765	1.752	1.765
r_{1C2C}	1.402	1.398	1.402	1.398	1.403(1.400)	1.398(1.395)
r_{2C3C}	1.394	1.389	1.394	1.389	1.393(1.395)	1.387(1.390)
r_{3C4C}	1.396	1.390	1.387	1.382	1.400(1.397)	1.396(1.393)
r_{2C8H}	1.082	1.081	1.081	1.081	1.082	1.081
r_{3C9H}	1.081	1.082	1.080	1.081	1.083	1.083
$r_{4C12(H/F/C)}$	1.081	1.081	1.348	1.352	1.502	1.506
α_{6C1C2C}	119.9	119.6	119.7	119.5	119.4	119.1
α_{1C2C3C}	119.7	119.8	120.2	120.3	119.8	120.0(119.9)
α_{2C3C4C}	120.6	120.7	118.9	119.0	121.6	121.7(121.8)
α_{1C2C8H}	120.1	120.2	120.2	120.3	120.1	120.2(120.3)
α_{4C3C9H}	120.1	120.1	119.8	119.9	119.5(119.4)	119.6(119.5)

[a]*p*-CH_3-$C_6H_4S\cdot$ of molecular symmetry C_s can have two different values for each pair of bond lengths and angles in contrast with C_{2v} symmetry. These values are shown in parentheses. [b]The DFT calculation has been carried out using B3LYP functional

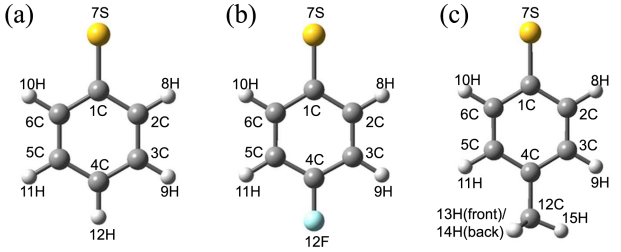

Figure 1. Molecular structures of the (a) $C_6H_5S\cdot$, (b) *p*-F-$C_6H_4S\cdot$ and (c) *p*-CH_3-$C_6H_4S\cdot$.

Vertical energy gap is calculated to be 0.400 eV by CASPT2 for $C_6H_5S\cdot$ which is 0.033 eV higher than the adiabatic energy gap, suggesting that the structural change of the aromatic ring moiety upon electronic excitation should be quite significant. Generally, it is found that SA-CASSCF (0.285 eV) and MRCI+Q (0.325 eV) predictions underestimate the adiabatic $\tilde{A}$-$\tilde{X}$ energy gap whereas it is overestimated by a DFT value of 0.384 eV. Upon *para*-substitution of F and CH_3 on the aromatic ring moiety, the adiabatic $\tilde{A}$-$\tilde{X}$ energy gap is calculated to be increased by 0.040 (323 cm^{-1}) or 0.039 (315 cm^{-1}) eV, respectively, according to the CASPT2/aug-cc-pVTZ calculation. Similarly, calculations with other methods also predict the larger $\tilde{A}$-$\tilde{X}$ energy gap for *p*-F-$C_6H_4S\cdot$ and *p*-CH_3-$C_6H_4S\cdot$ compared to that of $C_6H_5S\cdot$, Table 2. SA-CASSCF (or MRCI+Q) gives 202 (282) or 177 (242) cm^{-1} for F and CH_3 substitution, respectively, for the increase of the $\tilde{A}$-$\tilde{X}$ energy gap, which is smaller than that predicted by CASPT2. On the other hand, DFT gives 492 or 444 cm^{-1} upon F or CH_3 *para*-substitution, respectively. The increase in the adiabatic $\tilde{A}$-$\tilde{X}$ energy gap upon *para*-substitution is predicted to be slightly larger for F compared to CH_3 from all of four calculation methods. This trend is somewhat less straightforward to understand as the CH_3 group is believed to be the stronger electron donor compared to F (*vide infra*). Though CASPT2 seems to be most consistent with the experiment for $C_6H_5S\cdot$, it will be quite intriguing to investigate which method would be more appropriate for explaining the effect of *para*-substitution as different quantum mechanical methods have their own advantages in different circumstances.

Qualitative description for the origin of the structural and energetic changes of thiophenoxyl radicals upon chemical substitution can be given based on the charge and spin den-

Table 2. Theoretically obtained vertical excitation energies and adiabatic excitation energies for the $\tilde{X}\ ^2B_1/A''$ and $\tilde{A}\ ^2B_2/A'$ electronic states of the substituted thiophenoxyl radicals calculated using the SA-CASSCF, CASPT2, MRCI+Q, and DFT methods. Units are eV

	$\tilde{A}\ ^2B_2/A' \leftarrow \tilde{X}\ ^2B_1/A''$ Excitation energies	
	vertical	adiabatic
	$C_6H_5S\cdot$	
SA-CASSCF	0.354	0.285
CASPT2	0.400	0.367
MRCI+Q	0.376	0.325
DFT	0.416	0.384
Exp[15]	0.3719	
	p-F-$C_6H_4S\cdot$	
SA-CASSCF	0.383	0.310
CASPT2	0.448	0.407
MRCI+Q	0.419	0.360
DFT	0.487	0.445
	p-CH_3-$C_6H_4S\cdot$	
SA-CASSCF	0.388	0.307
CASPT2	0.446	0.406
MRCI+Q	0.415	0.355
DFT	0.477	0.439

Table 3. Mulliken and NBO charge densities for the $\tilde{X}$ and $\tilde{A}$ state of substituted thiophenoxyl radicals obtained from DFT calculation at the aug-cc-pVTZ basis level. See Figure 1 for the representative atom labels

	$C_6H_5S\cdot$		*p*-F-$C_6H_4S\cdot$		*p*-CH_3-$C_6H_4S\cdot$	
	Mulliken	NBO	Mulliken	NBO	Mulliken	NBO
			$\tilde{X}\ ^2B_1/A''$			
1C	0.512	-0.242	0.436	-0.255	0.506	-0.245
2C	-0.696	-0.164	-0.505	-0.147	-0.545(-0.707)	-0.155(-0.157)
3C	-0.340	-0.209	-0.615	-0.269	-0.749(-0.801)	-0.215(-0.213)
4C	-0.272	-0.154	0.716	0.439	1.340	0.034
7S	-0.365	0.079	-0.371	0.074	-0.385	0.062
8H	0.475	0.218	0.552	0.222	0.485(0.461)	0.217
9H	0.421	0.210	0.403	0.227	0.218(0.377)	0.206
12H/12F/12C	0.404	0.207	-0.454	-0.323	-0.769	-0.606
			$\tilde{A}\ ^2B_2/A'$			
1C	0.666	-0.227	0.576	-0.243	0.704	-0.234
2C	-0.818	-0.229	-0.629	-0.208	-0.667(-0.805)	-0.220(-0.218)
3C	-0.272	-0.180	-0.549	-0.244	-0.717(-0.786)	-0.185(-0.183)
4C	-0.359	-0.220	0.662	0.384	1.310	-0.035
7S	-0.289	0.229	-0.285	0.230	-0.303	0.222
8H	0.480	0.209	0.545	0.212	0.470(0.451)	0.208(0.207)
9H	0.398	0.206	0.391	0.223	0.207(0.357)	0.202
12H/12F/12C	0.405	0.206	-0.470	-0.337	-0.776	-0.596

Table 4. Mulliken and NBO spin densities for the $\tilde{X}$ and $\tilde{A}$ state of substituted thiophenoxyl radicals obtained from DFT calculation at the aug-cc-pVTZ basis level. See Figure 1 for the representative atom labels

	$C_6H_5S\cdot$		*p*-F-$C_6H_4S\cdot$		*p*-CH_3-$C_6H_4S\cdot$	
	Mulliken	NBO	Mulliken	NBO	Mulliken	NBO
			$\tilde{X}\ ^2B_1/A''$			
1C	-0.071	-0.072	-0.060	-0.065	-0.067	-0.065
2C	0.127	0.145	0.125	0.138	0.134(0.114)	0.146(0.134)
3C	-0.070	-0.069	-0.070	-0.062	-0.072(-0.071)	-0.066
4C	0.176	0.179	0.158	0.157	0.188	0.177
7S	0.798	0.752	0.778	0.741	0.779	0.733
8H	-0.008	-0.005	-0.005	-0.005	-0.008(-0.007)	-0.005(-0.004)
9H	0.002	0.002	0.002	0.002	0.005(0.004)	0.002
12H/12F/12C	-0.006	-0.005	0.021	0.021	-0.017	-0.008
			$\tilde{A}\ ^2B_2/A'$			
1C	-0.074	-0.022	-0.081	-0.022	-0.058	-0.022
2C	0.013	0.013	0.018	0.013	0.007(0.011)	0.013(0.014)
3C	0.022	0.003	0.026	0.003	0.027(0.029)	0.003
4C	-0.003	-0.003	0.001	-0.003	-0.005	-0.003
7S	1.069	0.993	1.069	0.993	1.061	0.993
8H	-0.030	-0.001	-0.037	-0.001	-0.034(-0.037)	-0.001
9H	-0.001	0.001	-0.001	0.001	0.001(-0.001)	0.001
12H/12F/12C	-0.001	0.000	0.001	0.000	0.000	0.000

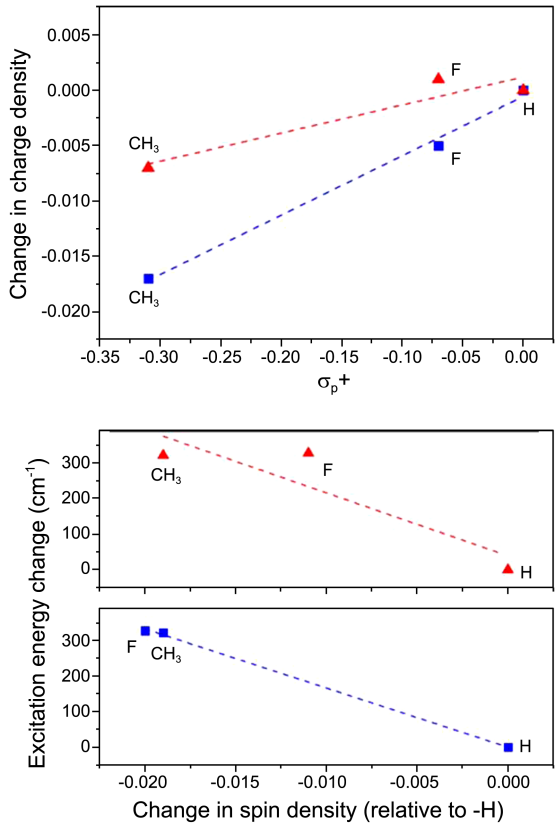

Figure 2. (Left) Plot of the calculated change in NBO charge density of the sulfur atom as a function of the σ_p^+ constant of the *para*-substituent for the $\tilde{X}$ (■) and $\tilde{A}$ (▲) state. The more negative value of σ_p^+, the stronger electron donating ability. The Mulliken charge is not shown for its similarity. (Right) Plot of the excitation energy change by *para*-substitution calculated using CASPT2 as a function of the change in spin density of the sulfur atom. The spin densities from the both NBO (▲) and Mulliken (■) population analysis give good correlations.

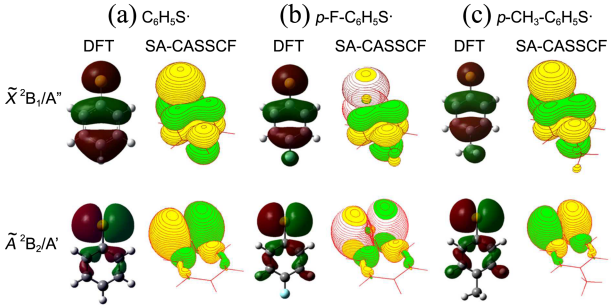

Figure 3. DFT SOMOs generated by B3LYP and SA-CASSCF SOMOs associated with electronically ground states (upper panel) and excited states (lower panel) for (a) $C_6H_5S\cdot$, (b) *p*-F-$C_6H_4S\cdot$ and (c) *p*-CH_3-$C_6H_4S\cdot$. The orbitals were visualized using Gauss View and MOLDEN respectively with an isovalue of 0.020.

sity distributions calculated by Mulliken[29] or NBO analysis, Tables 3 and 4. Absolute values are less reliable as those population analyses are not theoretically strict, and only qualitative trends should be taken to be meaningful. According to the Mulliken analysis by DFT/aug-cc-pVTZ, the partial charge on the sulfur atom decreases as F or CH_3 is being substituted on the *para*-position for the ground state. Even though NBO analysis gives the positive value for the charge density on sulfur, it also shows the decrease for the ground state thiophenoxyl radicals as electron donating groups are being substituted on the ring. This behavior is quite perceivable considering the Hammett-Brown polar substituent constant (σ_p^+)[30] of F and CH_3 as the linear dependence is observed when the change of S charge density is plotted versus σ_p^+, Figure 2. For excited states of thiophenoxyl radicals, however, the charge density on sulfur by Mulliken or NBO is decreased by the CH_3 substitution while it is slightly increased by the F substitution, suggesting that

the electron-donating effect of F or CH_3 is not manifested for the excited state. The more consistent behavior could be found by the spin density calculations, Table 4. The spin density is calculated to be localized on sulfur for both ground and excited states of all thiophenoxyl radicals studied in this work from both Mulliken and NBO analyses. Especially, for excited states, the spin density is found to be localized solely on sulfur, and it is little changed by the F or CH_3 *para*-substitution.

On the other hand, the S spin density of 0.798 (0.752) of $C_6H_5S\cdot$ decreases to 0.778 (0.741) and 0.779 (0.733), respectively, for *p*-F-$C_6H_4S\cdot$ and *p*-CH_3-$C_6H_4S\cdot$ in the ground state

Table 5. Harmonic vibrational frequencies for the $\tilde{X}$ and $\tilde{A}$ state of $C_6H_5S\cdot$, *p*-F-$C_6H_4S\cdot$ and *p*-CH_3-$C_6H_4S\cdot$ obtained using DFT. All units are cm^{-1}

mode	symmetry	$C_6H_5S\cdot$		*p*-F-$C_6H_4S\cdot$[a]		*p*-CH_3-$C_6H_4S\cdot$[a]	
		$\tilde{X}$	$\tilde{A}$	$\tilde{X}$	$\tilde{A}$	$\tilde{X}$	$\tilde{A}$
ν1	A_1 (A')	3103	3096	3109	3102	3098	3083
ν2		3091	3082	1221	1211	1194	1193
ν3		3072	3066	3095	3081	3068	3058
ν4		1546	1569	1552	1577	1559	1585
ν5		1439	1458	1450	1470	1452	1472
ν6		1162	1169	1139	1144	1169	1174
ν7		1048	1064	1046	1062	1046	1061
ν8		1009	1015	994	999	1001	1004
ν9		977	981	810	806	789	784
ν10		709	685	640	611	636	610
ν11		414	397	372	361	377	364
ν12	A_2 (A")	971	956	960	941	971	953
ν13		826	822	798	798	819	816
ν14		373	408	385	420	378	411
ν15	B_1 (A")	984	974	953	927	958	931
ν16		922	885	833	812	810	789
ν17		750	724	708	690	702	698
ν18		666	683	501	492	483	480
ν19		450	463	299	319	271	288
ν20		156	174	108	120	104	113
ν21	B_2 (A')	3100	3086	3107	3101	3096	3082
ν22		3081	3072	3096	3083	3064	3061
ν23		1529	1553	1528	1563	1506	1539
ν24		1418	1417	1387	1375	1390	1377
ν25		1302	1313	1272	1285	1287	1299
ν26		1261	1252	1257	1247	1258	1247
ν27		1142	1145	411	403	362	347
ν28		1062	1063	1077	1084	1098	1104
ν29		603	610	617	621	623	629
ν30		288	237	258	215	244	207
ν31	A'					3009	3003
ν32	A"					2970	2972
ν33	A'					2928	2929
ν34	A'					1440	1447
ν35	A"					1437	1441
ν36	A'					1370	1372
ν37	A"					1026	1034
ν38	A'					972	973
ν39	A"					47	28

[a]The numbering of *p*-F-$C_6H_4S\cdot$ and *p*-CH_3-$C_6H_4S\cdot$ vibrational modes map through from the corresponding normal modes of the $C_6H_5S\cdot$ radical.

according to Mulliken (NBO) analysis. The decrease of the S spin density with F or CH_3 substitution for the ground state of thiophenoxyl radical is quite similar, and this indeed correlates well with the behavior of the adiabatic $\tilde{A}$ - $\tilde{X}$ energy gap with chemical substitution, Figure 2. That is, the spin density on sulfur becomes delocalized with F or CH_3 *para*-substitution by the same extent for the ground state of thiophenoxyl radicals, whereas it is little affected by the chemical substitution in the excited state. Therefore, the stabilization of the ground state through spin delocalization contributes to the increase of the adiabatic $\tilde{A}$ - $\tilde{X}$ energy gap with F or CH_3 substitution. The importance of spin delocalization in energetics of substituted phenoxyl radicals had been reported by Fehir *et al*.,[31] and our findings here are quite consistent. Orbital shapes of singly-occupied molecular orbitals (SOMO) for ground and excited states of $C_6H_5S\cdot$, *p*-F-$C_6H_4S\cdot$, and *p*-CH_3-$C_6H_4S\cdot$ radicals calculated by DFT or SA-CASSCF strongly suggest that SOMO is localized on sulfur in the excited state and both charge and spin densities are little affected by the F or CH_3 *para*-substitution, Figure 3. Harmonic vibrational frequencies of ground and excited states of $C_6H_5S\cdot$, *p*-F-$C_6H_4S\cdot$, and *p*-CH_3-$C_6H_4S\cdot$ radicals calculated by DFT-B3LYP/aug-cc-pVTZ are given in Table 5. A scale factor of 0.9687 was multiplied for all presented numbers, based on the comparison of the experimental and theoretical values for ground state of $C_6H_5S\cdot$.[32] The zero-point energy differences between $\tilde{A}$ and $\tilde{X}$ states are calculated to be very small, giving 18, 34, and 30 cm^{-1} for $C_6H_5S\cdot$, *p*-F-$C_6H_4S\cdot$, and *p*-CH_3-$C_6H_4S\cdot$ radicals, respectively.

Conclusion

We investigated here the chemical substitution effect on the energetics and structure of first electronically excited and ground states of thiophenoxyl radical. *Para*-substitution of F and CH_3 groups certainly increases the adiabatic $\tilde{A}$ - $\tilde{X}$ energy gap by 323 or 315 cm^{-1}, respectively, according to CASPT2 though other theoretical methods such as SA-CASSCF, MRCI+Q, or DFT give slightly different numbers. Our Mulliken or NBO analysis gives a hint that the spin density on sulfur, which becomes somewhat delocalized by the chemical substitution in the ground state, could be mainly responsible for the increase of the $\tilde{A}$ - $\tilde{X}$ energy gap as the spin density in the excited thiophenoxyl radical is solely localized on sulfur and little affected by *para*-substitution whatsoever. Geometrical and vibrational changes upon F or CH_3 *para*-substitution are less pronounced. Theoretical results presented here should be essential for the photodissociation studies of thiophenols or thioanisoles which are excellent chemical systems for interrogating conical intersection dynamics. Furthermore, because $\tilde{A}$ state of thiophenoxyl radical is quite unique in terms of energetics and spin property, it would be very exciting to investigate chemical reactivity of *p*-Y-$C_6H_4S\cdot$ ($\tilde{A}$) to be compared with that of *p*-Y-$C_6H_4S\cdot$ ($\tilde{X}$) of different Y groups. Photodissociation of thiophenols could certainly be

used for the controlled generation of Ã states of thiophenoxyl radicals for further exciting stereo-specific chemical reaction studies.

Acknowledgments. We appreciate financial support from Grants of National Research Foundation (2012-0005607, SRC 2012-0000779).

References

1. Tseng, C.-M.; Lee, Y. T.; Ni, C.-K. *The Journal of Chemical Physics* **2004**, *121*, 2459.
2. Ashfold, M. N. R.; Devine, A. L.; Dixon, R. N.; King, G. A.; Nix, M. G. D.; Oliver, T. A. A. *Proceedings of the National Academy of Sciences* **2008**, *105*, 12701.
3. Roberts, G. M.; Chatterley, A. S.; Young, J. D.; Stavros, V. G. *The Journal of Physical Chemistry Letters* **2012**, *3*, 348.
4. Tseng, C.-M.; Lee, Y. T.; Ni, C.-K. *The Journal of Physical Chemistry A* **2009**, *113*, 3881.
5. Hadden, D. J.; Williams, C. A.; Roberts, G. M.; Stavros, V. G. *Physical Chemistry Chemical Physics* **2011**, *13*, 4494.
6. King, G. A.; Oliver, T. A. A.; Ashfold, M. N. R. *The Journal of Chemical Physics* **2010**, *132*, 214307.
7. Montero, R.; Conde, A. P.; Ovejas, V.; Martinez, R.; Castano, F.; Longarte, A. *The Journal of Chemical Physics* **2011**, *135*, 054308.
8. Wei, J.; Kuczmann, A.; Riedel, J.; Renth, F.; Temps, F. *Physical Chemistry Chemical Physics* **2003**, *5*, 315.
9. Montero, R.; Conde, A. P.; Ovejas, V.; Fernandez-Fernandez, M.; Castano, F.; de Aldana, J. R. V.; Longarte, A. *The Journal of Chemical Physics* **2012**, *137*, 064317.
10. Cronin, B.; Nix, M. G. D.; Qadiri, R. H.; Ashfold, M. N. R. *Physical Chemistry Chemical Physics* **2004**, *6*, 5031.
11. Lim, J. S.; Lim, I. S.; Lee, K.-S.; Ahn, D.-S.; Lee, Y. S.; Kim, S. K. *Angewandte Chemie International Edition* **2006**, *45*, 6290.
12. Lim, J. S.; Lee, Y. S.; Kim, S. K. *Angewandte Chemie International Edition* **2008**, *47*, 1853.
13. Devine, A. L.; Nix, M. G. D.; Dixon, R. N.; Ashfold, M. N. R. *The Journal of Physical Chemistry A* **2008**, *112*, 9563.
14. Lim, J. S.; Kim, S. K. *Nat. Chem.* **2010**, *2*, 627.
15. Kim, J. B.; Yacovitch, T. I.; Hock, C.; Neumark, D. M. *Physical Chemistry Chemical Physics* **2011**, *13*, 17378.
16. Cheng, C.-W.; Lee, Y.-P.; Witek, H. A. *The Journal of Physical Chemistry A* **2008**, *112*, 11998.
17. Armstrong, D. A.; Sun, Q.; Schuler, R. H. *The Journal of Physical Chemistry* **1996**, *100*, 9892.
18. Bordwell, F. G.; Zhang, X.-M.; Satish, A. V.; Cheng, J. P. *Journal of the American Chemical Society* **1994**, *116*, 6605.
19. Borges dos Santos, R. M.; Muralha, V. S. F.; Correia, C. F.; Guedes, R. C.; Costa Cabral, B. J.; Martinho Simões, J. A. *The Journal of Physical Chemistry A* **2002**, *106*, 9883.
20. Chandra, A. K.; Nam, P.-C.; Nguyen, M. T. *The Journal of Physical Chemistry A* **2003**, *107*, 9182.
21. Fu, Y.; Lin, B.-L.; Song, K.-S.; Liu, L.; Guo, Q.-X. *Journal of the Chemical Society, Perkin Transactions 2* **2002**, 1223.
22. Klein, E.; Lukeš, V.; Cibulková, Z.; Polovková, J. *Journal of Molecular Structure: THEOCHEM* **2006**, *758*, 149.
23. Jonsson, M.; Lind, J.; Merenyi, G.; Eriksen, T. E. *Journal of the Chemical Society, Perkin Transactions 2* **1994**, 2149.
24. Dunning, J. T. H. *The Journal of Chemical Physics* **1989**, *90*, 1007.
25. Woon, D. E.; Dunning, J. T. H. *The Journal of Chemical Physics* **1994**, *100*, 2975.
26. Werner, H.-J.; Knowles, P. J.; Knizia, G.; Manby, F. R.; Schütz, M.; Celani, P.; Korona, T.; Lindh, R.; Mitrushenkov, A.; Rauhut, G.; Shamasundar, K. R.; Adler, T. B.; Amos, R. D.; Bernhardsson, A.; Berning, A.; Cooper, D. L.; Deegan, M. J. O.; Dobbyn, A. J.; Eckert, F.; Goll, E.; Hampel, C.; Hesselmann, A.; Hetzer, G.; Hrenar, T.; Jansen, G.; Köppl, C.; Liu, Y.; Lloyd, A. W.; Mata, R. A.; May, A. J.; McNicholas, S. J.; Meyer, W.; Mura, M. E.; Nicklaß, A.; O'Neill, D. P.; Palmieri, P.; Peng, D.; Pflüger, K.; Pitzer, R.; Reiher, M.; Shiozaki, T.; Stoll, H.; Stone, A. J.; Tarroni, R.; Thorsteinsson, T.; Wang, M. *Molpro, A Package of ab initio Programs*, Version 2010.1
27. Frisch, M. J.; Trucks, G. W.; Schlegel, H. B.; Scuseria, G. E.; Robb, M. A.; Cheeseman, J. R.; Scalmani, G.; Barone, V.; Mennucci, B.; Petersson, G. A.; Nakatsuji, H.; Caricato, M.; Li, X.; Hratchian, H. P.; Izmaylov, A. F.; Bloino, J.; Zheng, G.; Sonnenberg, J. L.; Hada, M.; Ehara, M.; Toyota, K.; Fukuda, R.; Hasegawa, J.; Ishida, M.; Nakajima, T.; Honda, Y.; Kitao, O.; Nakai, H.; Vreven, T.; Montgomery, J. A., Jr.; Peralta, J. E.; Ogliaro, F.; Bearpark, M.; Heyd, J. J.; Brothers, E.; Kudin, K. N.; Staroverov, V. N.; Kobayashi, R.; Normand, J.; Raghavachari, K.; Rendell, A.; Burant, J. C.; Iyengar, S. S.; Tomasi, J.; Cossi, M.; Rega, N.; Millam, J. M.; Klene, M.; Knox, J. E.; Cross, J. B.; Bakken, V.; Adamo, C.; Jaramillo, J.; Gomperts, R.; Stratmann, R. E.; Yazyev, O.; Austin, A. J.; Cammi, R.; Pomelli, C.; Ochterski, J. W.; Martin, R. L.; Morokuma, K.; Zakrzewski, V. G.; Voth, G. A.; Salvador, P.; Dannenberg, J. J.; Dapprich, S.; Daniels, A. D.; Farkas, Ö.; Foresman, J. B.; Ortiz, J. V.; Cioslowski, J.; Fox, D. J. *Gaussian 09*, Revision A.02, Gaussian, Inc.: Wallingford CT, 2009.
28. Reed, A. E.; Curtiss, L. A.; Weinhold, F. *Chemical Reviews* **1988**, *88*, 899.
29. Mulliken, R. S. *The Journal of Chemical Physics* **1955**, *23*, 1833.
30. Hansch, C.; Leo, A.; Taft, R. W. *Chemical Reviews* **1991**, *91*, 165.
31. Fehir, J. R. J.; McCusker, J. K. *The Journal of Physical Chemistry A* **2009**, *113*, 9249.
32. Merrick, J. P.; Moran, D.; Radom, L. *The Journal of Physical Chemistry A* **2007**, *111*, 11683.